

Date of submission March 5, 2020

Digital Object Identifier 10.1109/ACCESS.2017.DOI

Segmentation of Satellite Imagery using U-Net Models for Land Cover Classification

PRIIT ULMAS¹, INNAR LIIV^{1,2}¹Department of Software Science, Tallinn University of Technology, Akadeemia Tee 15a, 12618 Tallinn, Estonia (e-mail: innar.liiv@taltech.ee, priit.ulmas@gmail.com)²Centre for Technology and Global Affairs, University of Oxford, Manor Road, Oxford OX1 3UQ, United Kingdom

Corresponding author: Priit Ulmas (e-mail: priit.ulmas@gmail.com).

arXiv:2003.02899v1 [cs.CV] 5 Mar 2020

ABSTRACT The focus of this paper is using a convolutional machine learning model with a modified U-Net structure for creating land cover classification mapping based on satellite imagery. The aim of the research is to train and test convolutional models for automatic land cover mapping and to assess their usability in increasing land cover mapping accuracy and change detection. To solve these tasks, authors prepared a dataset and trained machine learning models for land cover classification and semantic segmentation from satellite images. The results were analysed on three different land classification levels. BigEarthNet satellite image archive was selected for the research as one of two main datasets. This novel and recent dataset was published in 2019 and includes Sentinel-2 satellite photos from 10 European countries made in 2017 and 2018. As a second dataset the authors composed an original set containing a Sentinel-2 image and a CORINE land cover map of Estonia. The developed classification model shows a high overall F_1 score of 0.749 on multiclass land cover classification with 43 possible image labels. The model also highlights noisy data in the BigEarthNet dataset, where images seem to have incorrect labels. The segmentation models offer a solution for generating automatic land cover mappings based on Sentinel-2 satellite images and show a high IoU score for land cover classes such as forests, inland waters and arable land. The models show a capability of increasing the accuracy of existing land classification maps and in land cover change detection.

INDEX TERMS Satellite Imagery, U-Net Models, Land Cover Classification.

I. INTRODUCTION

WE are witnessing rapid development in space technologies both in physical satellite deployments and in data processing capabilities. The growing number of earth observation (EO) satellites produce an expanding amount of data, which requires a set of tools supported by artificial intelligence to process and extract information from [1]. This paper looks at deep convolutional neural networks (CNN) in a study of pixel level land cover classification mapping from satellite images.

Land cover mapping is a highly important tool for monitoring both the environmental development for regional planning as well as detecting changes in the environment. One such use case is monitoring UN Sustainable Development Goals (SDGs) [2] [3], specifically goal 15: Life on Land.

However, the current large-scale land cover maps have several weaknesses, most notably the complicated, labour inten-

sive and time-consuming process of creating them. Preparing such maps often requires people from the local areas to validate and classify the data. And even though a lot of effort is put into creating the maps, they provide a relatively low spatial accuracy which is not sufficient for automated change detection of small-scale changes. The CORINE Land Cover (CLC) map, for example, has been created with a 6-year interval. The most recent one, 2018 version, had a production time of 1.5 years [4].

When looking at ways of automatic change detection, for example in forestry mapping deforestation and illegal logging activity, a more precise and faster land cover mapping process is needed to detect and highlight small scale changes happening in weekly or even daily time frames.

Deep learning has shown high accuracy in computer vision tasks and has high potential to handle the growing amount of Earth Observation (EO) data in an automated process

[5]. For generating land cover classification maps an image segmentation task needs to be solved. Pixel level segmentation on satellite images is challenging because collecting a ground truth dataset for training such a segmentation model is difficult and time consuming.

Fortunately, a transfer learning approach can be taken, where a model trained for one task is repurposed to solve a new task. Specifically, in this work we use a large scale classification dataset (BigEarthNet) to develop a classification model and then repurpose this learning in a segmentation model.

The solution to this research problem is split into two tasks. Firstly, to create a land cover classification model using a large-scaled BigEarthNet dataset and secondly, to use this model as a pretrained encoder in a modified U-Net model to generate pixel level land cover classification maps, using a much smaller dataset for training. In the first task we benefit from the large dataset to learn the features of satellite images - the model will become good in reading satellite images. As in the second task we have a lot smaller dataset with more noise, we benefit from using a transfer learning approach to carry on the ability to read satellite images we trained in the first model.

The remainder of this paper is organized as follows. In Section II, we introduce additional background and discuss the topics addressed in this paper. In Section III, we look at the approach taken in this work. In Section IV, we see a summary of the machine learning training process and Section V describes the results. Finally, Section VI concludes the paper by summarizing the results and indicating issues to be addressed in future work.

II. RELATED WORK

The use of deep convolutional models has proven to deliver superior accuracy in a large variety of computer vision tasks and so also in satellite image understanding. One of the main bottlenecks in this approach has been the lack of labelled training data, which needs to be manually collected and prepared. In the case of image segmentation, the pixel level segmentation masks are even more difficult to collect. [5]

One way to overcome the lack of training data is to use a weakly supervised learning method. This has been recently employed by [6] and [7]. Weakly supervised approaches aim to overcome the need for complex training datasets, which in many cases do not exist and are difficult to create. Nivaggioli *et al.* [6] used an approach suggested by [8] on satellite imagery. Wang *et al.* [7] explore weak labels in the form of a single pixel label per image and class activation maps to create pixel level land cover mappings.

Automated land cover mapping is an active field of research with many machine learning approaches suggested, solving tasks such as vegetation extraction [9] or land cover change detection [10]. In creating a global land cover map, CORINE [11] uses several data fusion and pre-processing steps together with ancillary data sources to generate a training dataset. A rule-based approach combined with decision

tree models is then applied to create a land cover map. To overcome the lack of large-scale image datasets for model training transfer learning and data augmentation methods are used [12] [13].

Different satellite data sources have been applied for automatic land cover detection. For land cover and crop type classification [14] used Sentinel-1A and Landsat-8 data. In [15], Sentinel-1 and Sentinel-2 data is used in a multi-source approach to benefit from combining radar and optical data as a time series.

In this work, firstly, a land cover classification model is created using the large-scale BigEarthNet dataset, followed by creating a modified U-Net model using a transfer learning approach. CORINE Land Cover data of 2018 is then used as a training set for the segmentation model and data augmentation is used in the model training process.

III. METHODOLOGY

This chapter describes the main data pre-processing steps and the neural network architectures used.

A. DATA PREPARATION

Two data sources were used to train machine learning models. In the first stage BigEarthNet [16] was used to solve the classification task. Secondly, an original custom dataset was created to train the segmentation model for the semantic segmentation task.

1) BigEarthNet dataset

BigEarthNet is a large-scale Sentinel-2 dataset collected from a total of 125 Sentinel-2 tiles covering areas of 10 countries in Europe. The dataset was prepared with data from 2017 and 2018, and it was published in 2019. A total of 590 326 tiles of size 120 x 120px are annotated with land cover classification labels according to the third level of CORINE land cover classification covering a total of 43 different land cover classes. [16]

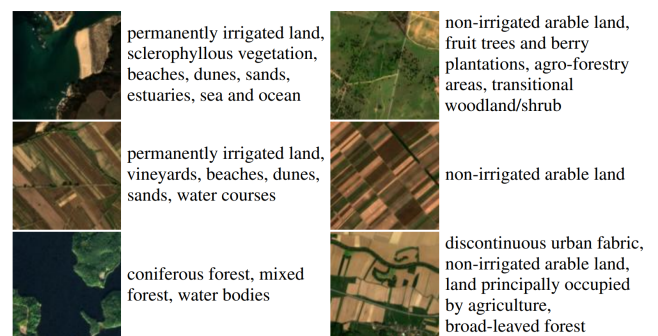


FIGURE 1. An example from the BigEarthNet dataset showing individual satellite images and corresponding image labels. [16]

In pre-processing a total of 70 987 images with cloud coverage or snow [16] were left out of the data and the remaining was split into training and test sets. An 80% subset

TABLE 1. CORINE Land cover classification labels. A three-level hierarchical classification structure is indicated by the first column.

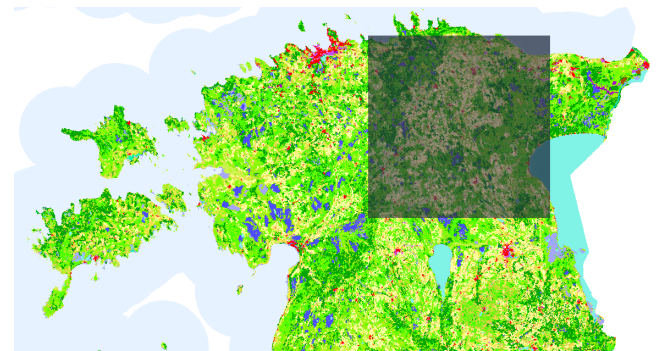
Code	Land Cover Category	Images
1	Artificial surfaces	
11	Urban fabric	
111	Continuous urban fabric	10 784
112	Discontinuous urban fabric	69 872
12	Industrial, commercial and transport units	
121	Industrial or commercial units	12 895
122	Road and rail networks and associated land	3 384
123	Port areas	509
124	Airports	979
13	Mine, dump and construction sites	
131	Mineral extraction sites	4 618
132	Dump sites	959
133	Construction sites	1 174
14	Artificial, non-agricultural vegetated areas	
141	Green urban areas	1 786
142	Sport and leisure facilities	5 353
2	Agricultural areas	
21	Arable land	
211	Non-irrigated arable land	196 695
212	Permanently irrigated land	13 589
213	Rice fields	3 793
22	Permanent crops	
221	Vineyards	9 567
222	Fruit trees and berry plantations	4 754
223	Olive groves	12 538
23	Pastures	
231	Pastures	103 554
24	Heterogeneous agricultural areas	
241	Annual crops associated with permanent crops	7 022
242	Complex cultivation patterns	107 786
243	Land principally occupied by agriculture, with significant areas of natural vegetation	147 095
244	Agro-forestry areas	30 674
3	Forest and semi natural areas	
31	Forests	
311	Broad-leaved forest	150 944
312	Coniferous forest	211 703
313	Mixed forest	217 119
32	Scrub and/or herbaceous vegetation associations	
321	Natural grasslands	12 835
322	Moors and heathland	5 890
323	Sclerophyllous vegetation	11 241
324	Transitional woodland-shrub	173 506
33	Open spaces with little or no vegetation	
331	Beaches, dunes, sands	1 578
332	Bare rock	3 277
333	Sparsely vegetated areas	1 563
334	Burnt areas	328
4	Wetlands	
41	Inland wetlands	
411	Inland marshes	6 236
412	Peat bogs	23 207
42	Maritime wetlands	
421	Salt marshes	1 562
422	Salines	424
423	Intertidal flats	1 003
5	Water bodies	
51	Inland waters	
511	Water courses	10 572
512	Water bodies	83 811
52	Marine waters	
521	Coastal lagoons	1 498
522	Estuaries	1 086
523	Sea and ocean	81 612

of the data was used for training the classification model and the remaining 20% set was used for validation.

Additionally, the classification labels were formatted into three levels of classification, corresponding to the hierarchy of CORINE land cover classification (Table 1). [17]

2) Sentinel-2 and CORINE combined dataset

To train the segmentation model a custom dataset was combined from the CORINE Land Cover map (2018) and a Sentinel-2 satellite image. For the purposes of this research a single Sentinel-2 image was selected together with the corresponding land cover mapping (Fig. 2). Sentinel-2 tile: S2A_MSIL1C_20180510T094031_N0206_R036_T35VMF_20180510T114819

**FIGURE 2.** Square indicates the satellite image used for training the segmentation model.

The R, G, B channels of the satellite image were used in the case study, combined into a single .png image. Both the satellite image and the land cover map were then divided into 120 x 120px images, resulting in a dataset of 8281 image pairs.

The CORINE Land Cover classification has a three-level hierarchical structure [17] as shown in Table 1. The segmentation labels were also formatted into three separate sets corresponding to the hierarchy of land cover classification labels.

The created dataset is a small sample of satellite data and accounts for a smaller set of labels compared to the classification dataset. Where BigEarthNet has 5, 15 and 43 different land cover classes over three classification levels, the segmentation dataset has 5, 14 and 25 respectively. The main difference is therefore on the third level, where fewer classes are present.

An 80% subset of the data was used for training the segmentation model and the remaining 20% set was kept for validation. Understandably the much lower precision of the CORINE Land Cover map introduces noise into the segmentation dataset when raised to the higher resolution of a Sentinel-2 satellite image. This will also impact the accuracy results as a portion of this dataset is used for validation.

3) Dataset accuracy

The accuracy of the CORINE land cover map used in the segmentation dataset is estimated to be close to 85% [18]. The data accuracy is also defined by its Minimum Mapping Unit (MMU) of 25 ha for areas and 100 m for linear instances [17], resulting in a relatively high level of generalisation. This omitting of small features creates a noisy dataset for the convolutional model to train on and means that there is no high accuracy ground truth data to rely on or to measure model results on.

B. NETWORK ARCHITECTURE

Two neural network architectures were used in the case study. Firstly, a ResNet50 model [19] was used for the classification task. Secondly, the pretrained ResNet50 classification model was used as the encoder in the modified U-Net model [20] to solve the segmentation task. This transfer learning approach [21] allows us to use the learning gained in the first task to solve a new, more complex task where training data is difficult to acquire. In the case of traditional image recognition tasks, this might mean that a model previously trained on ImageNet [22] is used as a starting point. This model, already trained on a dataset of over 14 million images, is good at identifying different features on an image. To solve a new task only the final layers might need to be changed and trained in order to generate the required output at high accuracy.

1) Classification model

For the classification task a ResNet model architecture was chosen. This architecture uses a repeating pattern of layer blocks, with skip connections added to allow creating deeper networks while avoiding model performance degrading. This state-of-the-art model architecture also won the ImageNet Large Scale Visual Recognition Challenge (ILSVRC) in image classification in 2015. [19]

2) Segmentation model

For image segmentation a U-Net like model architecture is used. This type of model is comprised of two main parts. Firstly, the encoder half of the model is used to detect features on an image. This portion of the model carries out a down-sampling process, bringing the input image down to a small size feature matrix. Secondly, the decoder half constructs the model output using the features as input and carries out an up-sampling process to bring back the spatial information of the input image.

C. EVALUATION METRICS

In both tasks the model will be assessed based on a validation set made up of 20% of the data (103 867 images in classification and 1 656 images in segmentation). The following metrics are used in assessing the model results, described by [23] and [24].

To analyse the BigEarthNet dataset to understand its complexity two metrics are used. Firstly, cardinality shows the average number of labels per image.

$$Cardinality = \frac{1}{N} \sum_{i=1}^N |Y_i| \quad (1)$$

Secondly, density is a metric that shows the average number of image labels out of all possible labels in the dataset.

$$Density = \frac{1}{N} \sum_{i=1}^N \frac{|Y_i|}{|L|} \quad \text{where } |L| = \bigcup_{i=1}^N Y_i \quad (2)$$

The strictest measure used for classification is Exact Match Ratio (MR) (3), where only the images with all labels correctly predicted are considered correct. It is strict because partially correct results will be considered incorrect.

$$MR = \frac{1}{N} \sum_{i=1}^N I(Y_i = Z_i) \quad (3)$$

Precision metric (4) is used to see the rate of correct labels out of all predicted labels. It combines the True Positive (TP) and False Positive (FP) results:

$$Precision = \frac{TP}{TP + FP} \quad (4)$$

The recall metric (5) is used to measure the proportion of correct labels out of all predicted labels. It combines the True Positive (TP) and False Negative (FN) results:

$$Recall = \frac{TP}{TP + FN} \quad (5)$$

For the classification task the F_1 value (6) will be used for model assessment. The F-score combines precision and recall into a single metric. In the case of F_1 we are putting an equal weight on both of these metrics.

$$F_1 = \frac{2 * precision * recall}{(precision) + recall} \quad (6)$$

Segmentation accuracy is measured using overall accuracy (7) as well by using class based Jaccard Index values (8).

$$Segmentation\ accuracy = \frac{Correct\ pixels}{All\ pixels} \quad (7)$$

$$Jaccard\ Index = \frac{TP}{TP + FN + FP} \quad (8)$$

IV. EXPERIMENTS

A. TRAINING ENVIRONMENT

The machine learning models used in the research were prepared using the Fast.ai library [25]. Built on the Pytorch framework [26], this high-level library is created with the aim of simplifying state-of-the-art model creation in deep learning. For the current work it enables creating a U-Net like architecture from an existing convolutional model, such

as ResNet. The training was carried out on a virtual machine using Nvidia K80 and P100 graphics cards.

B. MODEL TRAINING

In the experiments a total of six models were trained and their results analysed. Firstly, three classification models were created, one for each level of CORINE Land Cover classification. The BigEarthNet dataset was used in training the models. Secondly, the three classification models were used as pretrained encoders for three U-Net like segmentation models. These models were then trained on the dataset created by the authors.

1) Classification model training

An ImageNet [22] pretrained ResNet50 model was used to create the classification models. A total of three classification models were trained, one for each land cover classification level.

The model was trained on the BigEarthNet dataset, with satellite images as input and land classification labels as output. As the model was pretrained at start, the training was carried out in two stages, firstly by keeping most of the layers frozen and only training the last layers, later by training the whole model.

The training was carried out in a total of 15 epochs (10 epochs training only the last layers of the model followed by 5 epochs with all layers unfrozen).

2) Segmentation model training

For the segmentation task three modified U-Net models were created using the previously trained classification model weights as pre-trained encoders. These models were then trained on the custom land cover segmentation dataset, taking as input a satellite image and as output a CORINE Land Cover map.

As the models are using a pretrained model as the encoder the training is carried out in two stages. Firstly, only the decoder is trained (5-10 epochs), followed by unfreezing all layers and training the whole model (5-10 epochs). A similar process is carried out for all three classification levels.

V. RESULTS

A. DATASET ANALYSIS

In analysis of BigEarthNet through the three levels of CORINE Land Cover classification two metrics were calculated - cardinality and density. These characteristics allow us to illustrate the multi-class and multi-label dataset. Results are shown in table 2.

TABLE 2. Cardinality and density of the BigEarthNet dataset.

Classification level	Cardinality	Density
Level 1	1.78	0.357
Level 2	2.48	0.165
Level 3	2.96	0.069

From the results we can see that from the first to the third level of classification the cardinality rises from 1.78 to 2.96, meaning that between the first and third levels the average number of labels for an image roughly doubles. However, from density the complexity rises more, choosing the labels out of all possible choices becomes nearly five times more difficult (cardinality reducing from 0.357 on the first level down to 0.069 on the third level).

Both of the training datasets are strongly imbalanced on all classification levels, meaning that there are a few classes highly represented followed by many classes with less data. One question explored in the work was to understand if the higher representation of a class is resulting in a higher score for the class. When looking at the correlation between the number of pictures per class and the class based F_1 score we can see a correlation value of **0.59**, indicating a medium correlation between the two. On the segmentation task we looked at the total number of pixels per class and the IoU score of the class. In this case we also see a medium correlation value of **0.66**. This shows that in addition to the class being represented in the dataset the visual distinction of the class plays an important role.

B. OVERALL RESULTS

1) Classification

The classification model shows high overall results (Table 3) on all three land cover classification levels. While the exact match ratio, where all labels are correctly predicted, drops from 75.3% on the first level down to 33.1% on the third level the proportion of images where all predicted labels are incorrect rises from 0.8% to only 4.9% on the third level. F_1 score remains relatively high on all three levels, going down to 0.749 for the third level. This F_1 score on the third level is also an improvement over the F_1 score of 0.6759 reached by [16].

TABLE 3. Classification and segmentation results. Exact match ratio (MR) indicates complete accurate classification, Partial indicates images with partially correct predictions and Incorrect indicates images with no correct predicted labels.

	Classification				Segmentation
	MR	Partial	Incorrect	F_1	Accuracy
Level 1	75.3%	23.9%	0.8%	0.920	91.4%
Level 2	45.9%	52.1%	2.1%	0.823	75.8%
Level 3	33.1%	61.9%	4.9%	0.749	59.7%

2) Segmentation

The segmentation model shows a high 91.4% pixel-level accuracy on the first classification level with 75.8% and 59.7% on the second and third levels (Table 3). An example of segmentation model results and comparison to validation data can be seen on Figures 3 and 4.

C. CLASS BASED ACCURACY

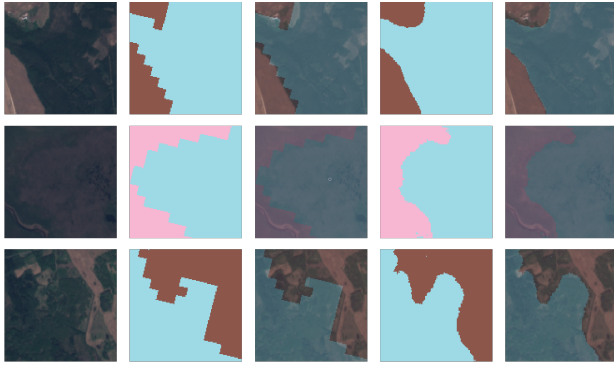


FIGURE 3. Segmentation results comparison. Satellite image tiles (column 1), existing land cover maps (column 2), segmentation results (column 4) and land cover map overlays (columns 3 and 5).

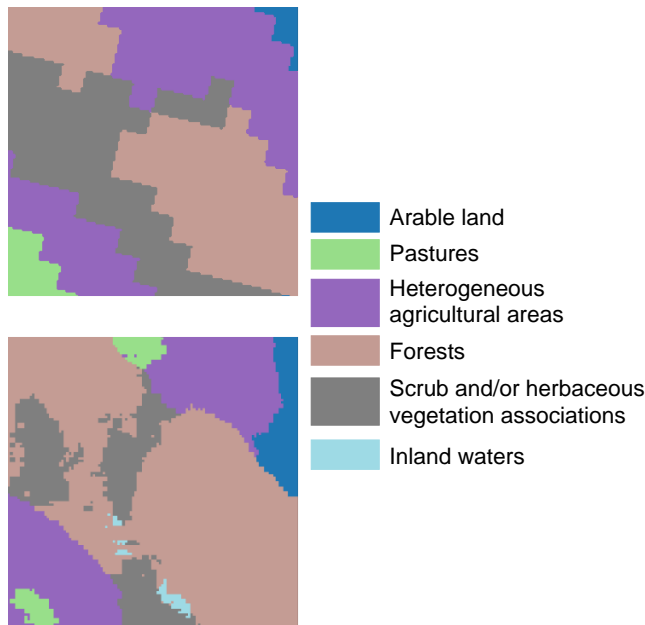


FIGURE 4. Example of segmentation results on the third level of classification (below) compared to the CORINE Land Cover map used in the validation set (above).

1) Classification

The classification results per class show high metrics on the first level and lower scores on the second and third levels, where the number of classes increases and visual separability of classes decreases.

On the first level (Table 4) we can see that the model performs the weakest on wetland areas (F_1 score 0.58) and artificial surfaces (F_1 score 0.77).

On the second level of classification (Table 5) we can see that most classes still show F_1 score above 0.5, with lower values only for industrial areas and scrub and/or herbaceous vegetation classes. These classes both have a small number of images and both can be difficult for the model to visually distinguish from other classes.

Looking at the third level of classification (Table 6) we see

TABLE 4. Classification level 1 results.

Class	Precision	Recall	F_1	Images
Agricultural areas	0.95	0.93	0.94	64 182
Artificial surfaces	0.85	0.71	0.77	17 689
Forests	0.94	0.95	0.95	70 138
Water bodies	0.95	0.91	0.93	28 570
Wetlands	0.85	0.45	0.58	4 869

TABLE 5. Classification level 2 results.

Class	Precision	Recall	F_1	Images
Urban fabric	0.87	0.85	0.86	38 755
Industrial, commercial, transport	0.74	0.11	0.20	1 299
Mine, dump, construction	0.93	0.94	0.94	64 364
Artificial, non-agri. vegetated areas	0.83	0.77	0.80	42 671
Arable land	0.73	0.44	0.55	3 050
Permanent crops	0.90	0.79	0.84	13 542
Pastures	0.84	0.45	0.58	4 424
Heterogeneous agricult. areas	0.99	0.98	0.98	15 083
Forests	0.84	0.42	0.56	455
Scrub and/or herbaceous vegetation	0.81	0.16	0.26	1 197
Open spaces, little or no vegetation	0.74	0.44	0.55	1 199
Inland wetlands	0.83	0.67	0.74	19 867
Maritime wetlands	0.75	0.43	0.54	4 968
Inland waters	0.75	0.59	0.66	31 820
Marine waters	0.83	0.72	0.77	15 118

that as the variety of classes increased nearly 3x between the second and third level the range of scores has spread to some classes missed completely (mineral extraction sites, sport and leisure facilities) and others reaching nearly maximum score (salt marshes, F_1 score 0.98).

2) Segmentation

Segmentation results at the first level of land cover classification show a high accuracy for the main land cover classes. This is also supported by visual comparison to the land cover map data used for validation (Figure 3).

On the first level of classification we can see from the confusion matrix (Figure 7) that the segmentation model performs well on three out of five classes.

On the second classification level (Figure 8) we can see that the strongest results come from arable land, forest and inland waters classes. From one side these are among the most represented classes by pixel count, but they are also visually distinct. Looking at the other classes we can see that many of them are visually not separable from RGB images and the results spread among visually similar classes.

The third level has the largest number of classes (25 are present in the segmentation dataset used for training and val-

TABLE 6. Classification level 3 results.

Class	Precision	Recall	F ₁	Images
Continuous urban fabric	0.81	0.76	0.78	6065
Discontinuous urban fabric	0.50	0.01	0.01	172
Industrial or commercial units	0.62	0.26	0.36	1408
Road and rail networks and associated land	0.73	0.52	0.61	549
Port areas	0.82	0.57	0.68	359
Airports	0.80	0.72	0.76	28 253
Mineral extraction sites	0.00	0.00	0.00	72
Dump sites	0.86	0.72	0.78	302
Construction sites	0.75	0.64	0.69	20 948
Green urban areas	0.86	0.86	0.86	32 765
Sport and leisure facilities	0.00	0.00	0.00	247
Non-irrigated arable land	0.80	0.67	0.73	2 255
Permanently irrigated land	0.83	0.69	0.76	13 238
Rice fields	0.83	0.07	0.12	153
Vineyards	0.70	0.45	0.55	223
Fruit trees and berry plantations	0.79	0.16	0.27	922
Olive groves	0.61	0.07	0.13	319
Pastures	0.72	0.39	0.51	2 410
Annual crops associated with permanent crops	0.83	0.10	0.17	1 079
Complex cultivation patterns	0.82	0.33	0.47	193
Land principally occupied by agriculture, with significant areas of natural vegetation	0.79	0.50	0.61	26 257
Agro-forestry areas	0.78	0.14	0.23	819
Broad-leaved forest	0.81	0.82	0.81	35 380
Coniferous forest	0.77	0.20	0.32	1 050
Mixed forest	0.76	0.31	0.44	2 226
Natural grasslands	0.87	0.82	0.84	36 743
Moors and heathland	0.73	0.29	0.42	2 489
Sclerophyllous vegetation	0.84	0.66	0.74	19 867
Transitional woodland-shrub	0.84	0.54	0.65	3 363
Beaches, dunes, sands	0.77	0.50	0.61	2 683
Bare rocks	0.68	0.30	0.41	88
Sparsely vegetated areas	0.68	0.49	0.57	725
Burnt areas	0.60	0.06	0.11	652
Glaciers and perpetual snow	0.76	0.43	0.55	90
Inland marshes	0.80	0.33	0.46	286
Peat bogs	0.82	0.38	0.52	2 218
Salt marshes	0.99	0.98	0.98	14 603
Salines	0.66	0.10	0.17	248
Intertidal flats	0.77	0.07	0.13	1 007
Water courses	0.73	0.55	0.63	29 479
Water bodies	0.77	0.25	0.38	1 889
Coastal lagoons	0.90	0.76	0.83	11 706
Estuaries	0.81	0.65	0.72	1 938
Sea and ocean	0.81	0.65	0.72	1 938

TABLE 7. Segmentation Confusion Matrix for the first classification level. Rows indicate true labels and columns indicate model predictions. Main diagonal shows class based correct prediction accuracy.

Labels	1	2	3	4	5
1. Artificial surfaces	0.42	0.42	0.16		
2. Agricultural areas	0.02	0.77	0.21		
3. Forests	0.01	0.11	0.86	0.02	
4. Wetlands		0.01	0.57	0.40	0.01
5. Water bodies		0.05	0.09	0.04	0.83

idation) and shows a wide distribution of results (Figure 9). The best performing classes are also understandably similar to the first two levels. Arable land, forests, water bodies and urban fabric being the highest performing classes. From the confusion matrix we can also see that some of the error is happening between bordering areas, such as urban fabric and green urban areas. This error to some extent was introduced into the dataset by using the CORINE Land Cover map at the higher resolution of satellite images. This type of error is described next.

D. NOISE IN DATASETS

Analysis of the classification model by viewing misclassified images with the highest loss indicates noise in the BigEarthNet data labels. Figure 5 shows one example of this, where the actual label seems to be incorrect. This method can be used further to improve the BigEarthNet dataset by correcting image labels.

Combining the Sentinel-2 tile with the CORINE Land Cover map to generate a segmentation dataset also generates noise (Figure 6). Firstly, the lower spatial resolution map is transposed to match a higher resolution satellite image. Secondly, the CORINE land cover map has an estimated accuracy of about 85% and it omits areas less than 25 hectares and linear instances less than 100m wide.

E. DISCUSSION

Firstly, we saw from analysing the BigEarthNet dataset how the complexity of the task increases between the three land cover classification levels. This is understandable for a hierarchical classification structure.

Training of the machine learning models was similar for all three levels of classification. In all cases the model training started with an ImageNet pretrained ResNet50 model. From there all classification models were trained 10-15 epochs, which was sufficient to see the model accuracy plateau.

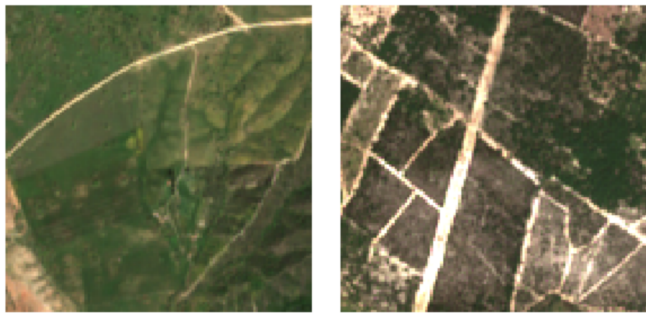
Training the segmentation models started with the trained classification models and a transfer learning method was used. The classification models were used as the encoders of the U-Net like architecture with the layers frozen during the first epochs. This allowed to first focus on training the decoder side of the model. After this all layers were trained in order to retrain the encoder side as well.

TABLE 8. Segmentation Confusion Matrix for the second classification level. Rows indicate true labels and columns indicate model predictions. Main diagonal shows class based correct prediction accuracy.

Labels	11	12	13	14	21	22	23	24	31	32	33	41	42	51	52
11. Urban fabric	0.42	0.03			0.17			0.29	0.09						
12. Industrial, commercial, transport	0.38	0.18	0.02		0.19			0.14	0.08	0.01					
13. Mine, dump, construction		0.06	0.13		0.16		0.03	0.08	0.31	0.2		0.01			0.03
14. Artificial, non-agricultural vegetated areas	0.34	0.06	0.07	0				0.11	0.4	0.01					
21. Arable land					0.76		0.07	0.05	0.12						
22. Permanent crops					0.07	0	0.32	0.16	0.29	0.15					
23. Pastures	0.01				0.36		0.28	0.11	0.22	0.01					
24. Heterogeneous agricult. areas	0.02				0.29		0.07	0.3	0.3	0.01					
31. Forests					0.05		0.01	0.03	0.87	0.03		0.01			
32. Scrub and/or herbaceous vegetation	0.01				0.04		0.02	0.05	0.67	0.16		0.05			
33. Open spaces, little or no vegetation									0.32		0			0.68	
41. Inland wetlands	0.01				0.01			0.01	0.32	0.18		0.46		0.01	
42. Maritime wetlands													0		
51. Inland waters								0.04	0.1			0.05		0.8	
52. Marine waters					0.01		0.01	0.04	0.05			0.02		0.51	0.36

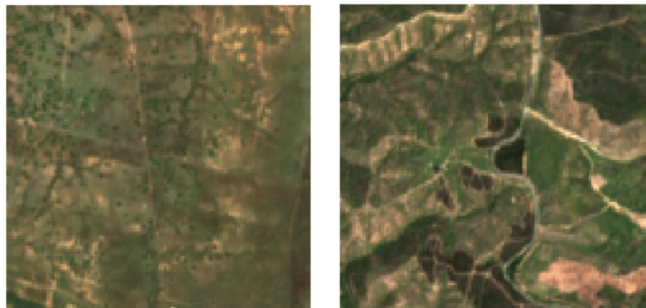
TABLE 9. Segmentation Confusion Matrix for the third classification level. Rows indicate true labels and columns indicate model predictions. Main diagonal shows class based correct prediction accuracy. Class labels as Table 1.

Labels	111	121	122	123	124	131	132	141	142	211	222	231	242	243	311	312	313	321	322	324	331	411	412	512	523	
111	0.48	0.02								0.2		0.01	0.21	0.02	0.05					0.01						
121	0.52	0.11				0.02				0.22			0.08	0.01	0.03					0.01						
122	0.14	0.01	0.06			0.01				0.21		0.03	0.23	0.11	0.07	0.12				0.01						
123				0																						
124	0.25	0.4			0	0.06				0.07			0.16		0.01					0.04						
131	0.02	0.04				0.08				0.29		0.02	0.05	0.1	0.09					0.26					0.06	
132	0.18	0.1				0.11	0			0.16			0.05	0.13	0.04					0.13		0.06		0.03		
141	0.5							0								0.5										
142	0.14	0.31				0.01			0				0.51							0.02						
211	0.01									0.79		0.08	0.03	0.01	0.01	0.07										
222										0.15	0	0.38	0.13			0.25				0.09						
231	0.01									0.42		0.29	0.08	0.01	0.03	0.14				0.02						
242	0.04									0.57		0.1	0.01	0.15	0.01	0.02	0.09									
243	0.04									0.28		0.08	0.26	0.03	0.04	0.24				0.02						
311	0.01									0.1		0.02	0.04	0.1	0.09	0.59				0.04						
312										0.03		0.01	0.02	0.01	0.49	0.39				0.05			0.01			
313										0.07		0.02	0.03	0.02	0.19	0.62				0.04						
321	0.03									0.08		0.2	0.13	0.05	0.05	0.32	0			0.08		0.05			0.01	
322										0.02		0.42	0.07	0.07	0.48			0								
324	0.01									0.05		0.03	0.05	0.03	0.18	0.43				0.18			0.04			
331														0.18							0	0.16		0.65	0.01	
411	0.02									0.02			0.03	0.03	0.13	0.25				0.26		0.09	0.16	0.02		
412													0.01	0.13	0.05					0.3			0.51			
512													0.05	0.04	0.04					0.01		0.03	0.03	0.66	0.14	
523										0.02			0.03	0.01	0.04					0.01		0.02		0.23	0.64	



(a) Predicted: Agro-forestry areas (Probability: 0.54), True label: Continuous urban fabric (Loss: 6.64).

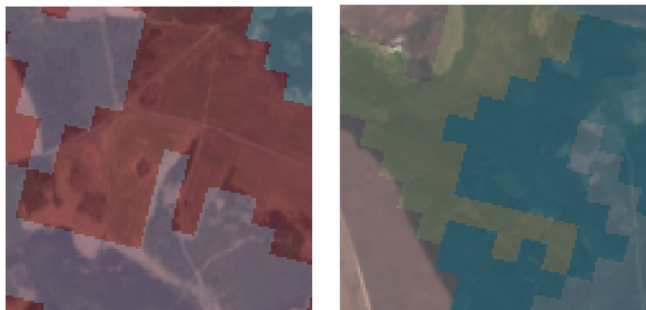
(b) Predicted: Coniferous forest (Probability: 0.78), True label: Continuous urban fabric (Loss: 6.86).



(c) Predicted: Agricultural areas (Probability: 0.89), True label: Artificial surfaces (Loss: 6.43).

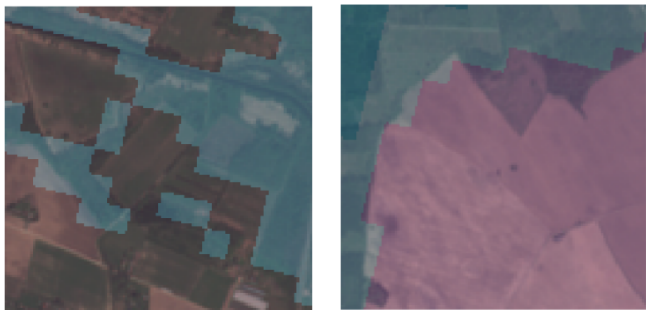
(d) Predicted: Broad-leaved forest (Probability: 0.67), True label: Continuous urban fabric (Loss: 7.65).

FIGURE 5. Noise in classification data. Possible incorrect labels indicated by high loss values.



(a)

(b)



(c)

(d)

FIGURE 6. CORINE Land Cover map overlaid on Sentinel-2 satellite image indicates noise in the segmentation dataset.

The classification models showed higher results on all three levels mainly for forest, agricultural areas and water bodies. With increasing the classification level, the complexity of the task increased and many smaller classes were added, which the model was not able to correctly classify.

When we look at misclassified results by the biggest loss, we can identify images which seem to have incorrect labels in the BigEarthNet dataset. Figure 5 shows examples of such images. Using the proposed classification model approach is a good way for identifying such mislabelled images for improving the dataset.

For all trained models the training was done until the accuracy metric reached a plateau and did not improve further. It can be possible to further improve the model by hyperparameter tuning and longer training, but this was sufficient for the current analysis.

Although the models show high result on some classes there are many smaller classes which show low results. One reason for this is understandably the fact that the data is imbalanced. From the results we can also see that visual distinction is an important factor as well. As we go to the 2nd and 3rd level of classification the visual distinction between the classes becomes smaller and some classes are not possible to determine on small scale images even for humans. One solution to this is to reduce the number of classes with a focus on usability in machine learning model training. This has been recently carried out for the BigEarthNet dataset in [27]. The third important factor is also the accuracy of training and validation datasets. The CORINE Land Cover map has been created with an aimed accuracy of 85% which contributes to the dataset noise. Also, the lower resolution of the land cover maps means that there is even more noise as the borders between different classes are less accurate compared to satellite images. This can be seen on Figure 6.

Considering the noise in the data described above it can be seen how the segmentation model in some cases is able to produce higher accuracy class borders. This also illustrates how the model is able to overcome the noise in the training data.

The process and machine learning models described in this work can be used for creating solutions in land monitoring and change detection. One such direction can be in monitoring changes in forest reserves, flagging deforestation logging activity. This is also part of UN Sustainable Development goals. Several further development directions have also been pointed out in the Conclusion section of this paper.

The classification ResNet model is also a good starting point for many other machine learning solutions based on satellite imagery. The model is trained on a large dataset and therefore has a good understanding of satellite image features. Depending on the problem it might only be needed to retrain the last layers of the model to solve a new task.

VI. CONCLUSION

The goal of this paper was to create machine learning models for classification and segmentation of satellite imagery with

the aim of improving existing land cover maps and land cover change detection.

A set of classification and segmentation models were created for satellite image classification and pixel level segmentation according to a three-level land cover category classification defined by the CORINE program. A novel BigEarthNet dataset was used, which is a public satellite imagery dataset for machine learning application. Also, a dataset was composed for training segmentation models, combining a Sentinel-2 satellite image of Estonia with the CORINE land cover map.

The results of this paper show the possibilities of using a convolutional neural network for this sort of task and underline the need for changing the land cover categories for achieving better accuracy. Also, as land cover is severely unbalanced, there is a need for class-based analysis and accuracy measurement, which was used in this work.

As an important additional result, the modified U-Net models showed a capability of improving on the existing low resolution of land cover maps (Figure 3). The models used existing map data as input and managed to offer up improved land cover mappings compared to the data used for validation.

The use of BigEarthNet and CORINE land cover datasets for machine learning highlighted some noise in the data, which affects the results. In BigEarthNet some images seem to be mislabelled and the authors suggest a method based on classification loss can be used to find the images for label correction. With land cover maps a limitation is its accuracy of 85%, a relatively low 100m resolution and the fact that distinctive areas under 25ha are not included on the map.

The goals of this paper were achieved and a total of six convolutional neural networks were created in order to analyse land cover classification and segmentation on three classification levels set by CORINE land cover mapping. In addition, several ideas for the improvement of the results and further research were proposed.

A. CONTRIBUTIONS OF THE PAPER

Contributions of this paper can be summarized as follows:

- A novel and very recent large-scale dataset, BigEarthNet, was used and state-of-the-art convolutional neural network architectures were applied in the research.
- Class based analysis of land cover classification and pixel level segmentation was carried out, highlighting the need for optimising the list of classes for machine learning purposes.
- An existing, manually created land cover dataset was used for machine learning model training. In visual comparison the created segmentation models showed results with higher accuracy than the dataset used for model training and validation.
- The research highlighted discrepancies in the BigEarthNet dataset and described a method for improving the dataset.

B. LIMITATIONS AND DIRECTIONS FOR FUTURE RESEARCH

This paper presented contributions, which can be further investigated from multiple interesting perspectives. Main current limitations and directions for future research can be summarized as follows:

- The accuracy of the CORINE Land Classification dataset, which was used in training and validation, was an important factor in the current results. A higher accuracy dataset will allow to increase the model accuracy and the reliability of model validation.
- Current work only used the red, green and blue channels of Sentinel-2 data. Including more channels allows for improving the results further. This data is available in BigEarthNet as well.
- Satellite data can be used for machine learning as a time series. This would allow to reinforce the land cover mapping confidence through time.
- The classification model approach can be used to flag and amend possible discrepancies in the BigEarthNet dataset. This can be done by viewing image classifications with high loss.
- The CORINE land cover classification used in this work is not optimal for machine learning based segmentation, we can see increased accuracy on some classes (forests, arable land, water bodies, for example) and we can see low results on classes which are visually less distinct. One direction for improving the results is to adjust the classes for better segmentation results. This approach has recently been carried out for the BigEarthNet dataset and a similar class selection could be used in image segmentation as well.
- The hierarchical structure of the CORINE land cover classification can be further utilised to improve the results. The results on the higher level can be used as a direction on the lower level.

Acknowledgement

This research was partially supported by IT Academy and Business Information Technology programs.

REFERENCES

- [1] "Towards a European AI for Earth Observation Research & Innovation Agenda," 2018, Proceedings of a workshop at ESA ϕ -lab. Accessed: Mar. 4, 2020. [Online]. Available: <http://blogs.esa.int/philab/files/2018/07/Towards-a-European-AI-for-Earth-Observation-Research-Innovation-Agenda-.pdf>
- [2] UN General Assembly, "Resolution Adopted by the General Assembly on 25 September 2015: 70/1." 2015. [Online]. Available: <https://undocs.org/A/RES/70/1>
- [3] K. Anderson, B. Ryan, W. Sonntag, A. Kavvada, and L. Friedl, "Earth observation in service of the 2030 agenda for sustainable development," *Geo-spatial Information Science*, vol. 20, no. 2, pp. 77–96, 2017.
- [4] Copernicus Programme. CORINE Land Cover. Accessed: Mar. 3, 2020. [Online]. Available: <https://land.copernicus.eu/pan-european/corine-land-cover>
- [5] C. D. Storie and C. J. Henry, "Deep learning neural networks for land use land cover mapping," *IGARSS 2018 - 2018 IEEE International Geoscience and Remote Sensing Symposium*, pp. 3445–3448, 07 2018.

- [6] A. Nivaggioli and H. Randrianarivo, "Weakly supervised semantic segmentation of satellite images," *CoRR*, vol. abs/1904.03983, 2019. [Online]. Available: <http://arxiv.org/abs/1904.03983>
- [7] S. Wang, W. Chen, S. M. Xie, G. Azzari, and D. B. Lobell, "Weakly supervised deep learning for segmentation of remote sensing imagery," *Remote Sensing*, vol. 12, no. 2, p. 207, 2020.
- [8] J. Ahn and S. Kwak, "Learning pixel-level semantic affinity with image-level supervision for weakly supervised semantic segmentation," *CoRR*, vol. abs/1803.10464, 2018. [Online]. Available: <http://arxiv.org/abs/1803.10464>
- [9] L. Zhiyong, L. Tongfei, J. Benediktsson, and H. Du, "A novel land cover change detection method based on k-means clustering and adaptive majority voting using bitemporal remote sensing images," *IEEE Access*, vol. PP, pp. 1–1, 01 2019.
- [10] Z. Zhan, Z. Xiaomeng, Y. Liu, X. Sun, C. Pang, and C. Zhao, "Vegetation land use/land cover extraction from high-resolution satellite images based on adaptive context inference," *IEEE Access*, vol. 8, pp. 1–1, 01 2020.
- [11] M. Buchhorn, B. Smets, L. Bertels, M. Lesiv, N.-E. Tsendbazar, M. Herold, and S. Fritz, "Copernicus Global Land Service: Land Cover 100m: epoch 2015: Globe," Oct. 2019. [Online]. Available: <https://doi.org/10.5281/zenodo.3243509>
- [12] G. Scott, M. England, W. Starns, R. Marcum, and C. Davis, "Training deep convolutional neural networks for land-cover classification of high-resolution imagery," *IEEE Geoscience and Remote Sensing Letters*, vol. PP, pp. 1–5, 02 2017.
- [13] Z. Benbahria, M. F. Smiej, I. Sebari, and H. Hajji, "Land cover intelligent mapping using transfer learning and semantic segmentation," 2019 7th Mediterranean Congress of Telecommunications (CMT), pp. 1–5, 10 2019.
- [14] N. Kussul, M. Lavreniuk, S. Skakun, and A. Shelestov, "Deep learning classification of land cover and crop types using remote sensing data," *IEEE Geoscience and Remote Sensing Letters*, vol. PP, pp. 1–5, 03 2017.
- [15] Y. J. E. Gbdjo, D. Ienco, L. Leroux, R. Interdonato, R. Gaetano, B. Ndao, and S. Dupuy, "Object-based multi-temporal and multi-source land cover mapping leveraging hierarchical class relationships," 2019.
- [16] G. Sumbul, M. Charfuelan, B. Demir, and V. Markl, "Bigearthnet: A large-scale benchmark archive for remote sensing image understanding," *IEEE International Conference on Geoscience and Remote Sensing Symposium*, pp. 5901–5904, Jul 2019. [Online]. Available: <http://dx.doi.org/10.1109/IGARSS.2019.8900532>
- [17] G. Büttner, J. Feranec, G. Jaffrain, L. Mari, G. Maucha, and T. Soukup, "The corine land cover 2000 project," *EARSeL eProceedings*, vol. 3, no. 3, p. 331, 2004.
- [18] SIRS SAS, France, "CORINE LAND COVER 2012 FINAL VALIDATION REPORT," Copernicus Land Monitoring Service, Tech. Rep., 2017, accessed: Jan. 3, 2020. [Online]. Available: <https://land.copernicus.eu/user-corner/technical-library/clc-2012-validation-report-1>
- [19] K. He, X. Zhang, S. Ren, and J. Sun, "Deep residual learning for image recognition," in *Proceedings of the IEEE Computer Society Conference on Computer Vision and Pattern Recognition*, vol. 2016-December. IEEE Computer Society, 12 2016, pp. 770–778.
- [20] O. Ronneberger, P. Fischer, and T. Brox, "U-net: Convolutional networks for biomedical image segmentation," in *Lecture Notes in Computer Science (including subseries Lecture Notes in Artificial Intelligence and Lecture Notes in Bioinformatics)*, vol. 9351. Springer Verlag, 2015, pp. 234–241.
- [21] C. Tan, F. Sun, T. Kong, W. Zhang, C. Yang, and C. Liu, "A survey on deep transfer learning," *CoRR*, vol. abs/1808.01974, 2018. [Online]. Available: <http://arxiv.org/abs/1808.01974>
- [22] O. Russakovsky, J. Deng, H. Su, J. Krause, S. Satheesh, S. Ma, Z. Huang, A. Karpathy, A. Khosla, M. Bernstein, A. C. Berg, and L. Fei-Fei, "ImageNet Large Scale Visual Recognition Challenge," *International Journal of Computer Vision (IJCV)*, vol. 115, no. 3, pp. 211–252, 2015.
- [23] M. S. Sorower, "A literature survey on algorithms for multi-label learning," 2010, accessed: Jan. 3, 2020.
- [24] F. C. Bernardini, R. B. Da Silva, E. Meza, and R. das Ostras-RJ-Brazil, "Analyzing the influence of cardinality and density characteristics on multi-label learning," *Proc. X Encontro Nacional de Inteligencia Artificial e Computacional-ENIAC 2013*, 2013.
- [25] J. Howard and S. Gugger, "Fastai: A layered api for deep learning," *Information*, vol. 11, no. 2, p. 108, Feb 2020. [Online]. Available: <http://dx.doi.org/10.3390/info11020108>
- [26] A. Paszke, S. Gross, F. Massa, A. Lerer, J. Bradbury, G. Chanan, T. Killeen, Z. Lin, N. Gimelshein, L. Antiga, A. Desmaison, A. Kopf, E. Yang, Z. DeVito, M. Raison, A. Tejani, S. Chilamkurthy, B. Steiner, L. Fang, J. Bai, and S. Chintala, "Pytorch: An imperative style, high-performance deep learning library," in *Advances in Neural Information Processing Systems 32*, H. Wallach, H. Larochelle, A. Beygelzimer, F. d'Alché-Buc, E. Fox, and R. Garnett, Eds. Curran Associates, Inc., 2019, pp. 8026–8037. [Online]. Available: <http://papers.nips.cc/paper/9015-pytorch-an-imperative-style-high-performance-deep-learning-library.pdf>
- [27] G. Sumbul, J. Kang, T. Kreuziger, F. Marcelino, H. Costa, P. Benevides, M. Caetano, and B. Demir, "Bigearthnet dataset with a new classification nomenclature for remote sensing image understanding," 2020. [Online]. Available: <http://arxiv.org/abs/2001.06372>



PRIIT ULMAS received the M.Sc. degree in civil engineering from Tallinn University of Technology, Tallinn, Estonia in 2013 and the second M.Sc. in business information technology from Tallinn University of Technology, Tallinn, Estonia in 2020.

He has over 10 years of industry engineering experience. Having previously worked on virtual design and construction and project management, he is currently working as a Machine Learning Engineer, developing automation solutions for manufacturing industry. His current research interests include image processing, machine learning, and computer vision.



INNAR LIIV received the Ph.D. degree from Tallinn University of Technology, Estonia. He was a Cyber Studies Visiting Research Fellow with the University of Oxford, from 2016 to 2017, a Visiting Scholar with Stanford University, in 2015, and a Postdoctoral Visiting Researcher with the Georgia Institute of Technology, in 2009. He is currently an Associate Professor of data science with the Tallinn University of Technology and a Research Associate with the Centre for Technology and Global Affairs, Oxford University. His research interests include e-government and data science, information visualization, and big data technology transfer to industrial and governmental applications. He is an IEEE Senior Member.

...